Published in final edited form as:
Neuroradiology. 2013 January ; 55(1): 65–70. doi:10.1007/s00234-012-1070-4.

Lack of aneurysm formation after carotid artery ligation in rabbits: a polymer MICROFIL® study

Daying Dai, **Yong Hong Ding**, **Ramanathan Kadirvel**, **Arash Ehteshami Rad**, **Debra A. Lewis**, and **David F. Kallmes**
Neuroradiology Research Laboratory, Department of Radiology, Mayo Clinic, 200 First Street SW, Rochester, MN 55905, USA

David F. Kallmes: kallmes.david@mayo.edu

Abstract

Introduction—Previous studies have noted formation of saccular aneurysms along the distal basilar artery/P1 segments after carotid ligation in rabbits. In this prospective study we employed MICROFIL®, a polymer, which was used to fill the entire arterial tree, to examine the incidence of micro-aneurysm formation following right common carotid artery (RCCA) ligation in rabbits.

Methods—RCCA ligation was performed in 18 New Zealand White rabbits for 0 day (*n*=2), 3 weeks (*n*=6), or 16 weeks (*n*=10). Three control rabbits without carotid surgery were sacrificed at 4 weeks. At the time of sacrifice, MICROFIL® MV-122 yellow was injected through left CCA to fill cerebral vasculature. After gross photographs were taken, specimens were embedded, sectioned, and stained for histopathological evaluation. Tissue and sections were carefully evaluated for microaneurysm formation, defined as a localized dilatation of the vessel wall, associated with fragmentation or complete loss of the internal elastic lamina (IEL), and/or medial degeneration.

Results—Gross examination with MICROFIL® opacification demonstrated no evidence of saccular aneurysm formation, but prominent perforating vessels were present in all 19 cases at, or adjacent to, the basilar terminus. Branches noted upon gross examination corresponded histologically to small, saccular contour defects, which demonstrated apparent loss of the IEL and apparent medial thinning. These observations, however, were a consequence of sectioning through the bases of perforating arteries, which simulated microaneurysm formation.

Conclusions—Unilateral carotid ligation does not induce microaneurysm formation at the basilar terminus in rabbits. Prominent perforating arteries as well as tissue injury from the processing may simulate “aneurysms” histologically.

Keywords

Aneurysm; Basilar terminus; Rabbit; MICROFIL®

Correspondence to: David F. Kallmes, kallmes.david@mayo.edu.

Data was presented at 49th American Society of Neuroradiology (ASNR) Annual Meeting and NER Foundation Symposium, June 2011, Seattle, USA.

Conflict of interest We declare that we have no conflict of interest.

Introduction

Multiple animal models [1–4] have been proposed in which carotid ligation, either alone or in combination with hypertension, leads to formation of microaneurysms around the Circle of Willis. These experimental aneurysms apparently form as a result of increased hemodynamic stress and are well described in mice and rats. Recently, similar studies [5] have been extended to rabbits where carotid ligation leads to apparent aneurysm formation along the P1 segments following uni- or bilateral carotid ligation. However, others have called into question the nature of these aneurysmal dilations noted in rabbits [6, 7], suggesting that these apparent aneurysms are, in fact, artifacts of histologic processing.

Previous studies of carotid artery ligation-induced rabbit aneurysms have relied exclusively on histologic analysis rather than vascular imaging or gross examination to detect aneurysms. As such, small branch vessels sectioned at their base might simulate a saccular aneurysm histologically [6]. Polymer impregnation of blood vessels affords an ideal mechanism to study the morphology of any type of arterial tree, including small branch arteries in rodent brains [8]. The purpose of the current study was to utilize polymer MICRO-FIL® technology to assess the three-dimensional structure of the rabbit intracranial vasculature following carotid ligation, in order to better define the presence and character of microaneurysms and other structures, including small, branch arteries, along the distal basilar artery/P1 segments.

Methods

Elastase-induced saccular aneurysms in right common carotid artery were created in 18 female New Zealand white rabbits for testing aneurysm devices. Detailed procedures for aneurysm creation have been described elsewhere [9, 10]. Three age-matched female New Zealand white rabbits without carotid surgery were included as controls. These rabbits had undergone renal angiography and embolization. After the rabbits were euthanized at the end of testing, the cerebral vessels were harvested and processed for the current basilar artery study. All animal surgeries and procedures were approved by the Institutional Animal Care and Use Committee at our institution.

MICROFIL® and tissue harvest

After the rabbit was euthanized, a 20 G catheter was placed in retrograde fashion in the left CCA and a small cut was made at the right jugular vein (RJV). Heparinized saline (100 U/ml) was continuously infused into the cannula, until the effluent from the RJV was light pink. Then the animals were perfusion-fixed through the 20 G catheter with 10 % buffered formalin for 5 min at a pressure of 150 mmHg followed by flush with heparinized saline for 5 min. Finally, 5 ml MICROFIL®1 MV 122 Yellow (Flow Tech; Carver, MA) was manually perfused through the 20 G catheter. The MICROFIL® was allowed to solidify for 1 h at room temperature. The Circle of Willis, along with the brain parenchyma, were harvested and fixed in 10 % buffered formalin for 24 h at room temperature. Under a dissection microscope (Leica MZ 125), gross inspection of the arterial tree was performed to determine presence and diameters of the posterior communicating arteries (PComms). In addition, special attention was paid to the basilar terminus and its branches. The Circle of Willis was photographed using the MicroPublisher 5.0 RTV camera attached to the dissection microscope. A small ruler, with 1.0 mm increments, was photographed along with the arteries for measurement calibration. After photography, the basilar artery and its branches were carefully dissected free from surrounding tissues and were fixed in 10 % formalin for further processing. Tissues were harvested at various time points following vessel ligation, including 0 day (n= 2), 3 weeks (n=6), and 16 weeks (n=10) for test subjects and 4 weeks after renal angiography and embolization (n=3) for control subjects.

Morphometry and analysis

The relative diameters of right and left PComms for each rabbit were measured using Image-Pro Plus software (Image-Pro Plus, Media Cybernetics, Inc). Diameters were compared using a Student *t* test (JMP, ver. 8.0, SAS Institute Inc, Cary, NC).

Histologic processing

The basilar artery and its branches were dehydrated in an ascending series of ethanol, cleared in xylene, and embedded in paraffin. They were then sectioned at 4 μm in a coronal orientation, to show the basilar bifurcation and its branches. The first section was collected when the investigator observed the bifurcation of basilar artery, and then serial sections (4 μm) were collected until the bifurcation disappeared.

All serial sections of each subject were stained with hematoxylin and eosin (H&E) for conventional pathological evaluation. After the H&E staining sections were evaluated and the photomicrographs were taken, if needed, the slides were placed in 70 % alcohol with 1 % HCl added to remove the H&E stain. This was followed by staining with Verhoeff Elastic Van Gieson. The sections were placed in Verhoeff's staining solutions for 15 min. They were rinsed in running distilled water for 10 min, after which they were differentiated in 2 % ferric chloride using the aid of a microscope. After being rinsed in running distilled water, the slides were rinsed in 95 % alcohol for 30 s, counter-stained in filtered Van Gieson's solution for 1 min 30 s. Finally, the slides were dehydrated in methanol and acetone, cleared in xylene, and mounted with Shandon EZ mount medium.

Histologic evaluation

One observer who was trained as a clinic pathologist, with more than 10 years experience in rabbit vascular histopathology, evaluated all the serial sections for the current study. The same investigator processed all the tissues for the current study.

For each subject, every serial section (totaling approximately 65 serial sections per subject) at the basilar terminus was reviewed to evaluate morphological change in the arterial wall. The following morphological changes were defined as microaneurysm formation: localized dilatation of the vessel wall associated with fragmentation or loss of the internal elastic lamina (IEL) with or without medial degeneration. All localized segments of the vessel wall satisfying the criteria for "aneurysmal changes" noted above were then evaluated further using both the gross pathologic findings from the MICROFIL® opacification images and serial histologic sections. The apparent "aneurysm" was co-localized on the MICROFIL® images to detect either saccular aneurysm formation or the presence of a branch artery. Further, we viewed serial histologic sections to determine whether the apparent "aneurysm" was, in fact, the origin of a branch artery.

In addition, the following histologic findings were defined as representing manual, mechanical damage of IEL from the processing and sectioning: sharp, localized IEL loss associated with adjacent, apparent tearing of the IEL and/or torn endothelial cells.

Results

Gross examination of MICROFIL® images demonstrated no evidence of saccular aneurysms in the basilar terminus area for either test subjects at 0 day, 3 weeks, and 16 weeks or control subjects. The local arterial wall at the basilar terminus appeared to be smooth and even, without evidence of local dilation or bulge in all rabbits (Fig. 1a–c). Prominent, perforating vessels were present at the basilar terminus area and/or close to the basilar terminus area in all 21 cases (Fig. 2a–b). The PComms were present and symmetrical

in all three control rabbits and the two rabbits at day 0 after right common carotid artery ligation. Mean diameter of the right and left PComms both were 0.40±0.06 mm (p=1.00) for the control subjects; they were 0.46±0.03 mm vs. 0.45±0.04 mm (p= 0.8) for the subjects at 0 day. The PComms were present and asymmetrically enlarged on the right side as compared to the left in all 16 test subjects at 3 and 16 weeks, indicating flow-induced enlargement and elongation of the PComm ipsilateral to the ligated right common carotid artery (RCCA). Mean diameter of the right and left PComms were 0.8±0.2 and 0.5 ±0.1 mm, respectively (p=.000003). The mean diameter of the right PComms was significantly larger than that of control subjects (0.8 vs. 0.4, p<.001). There was no difference in the diameters of left PComms between the test and control subjects (0.5 vs. 0.4, p=0.15).

Small branches that were noted in the gross MICROFIL® examination corresponded histology to small, saccular contour defects. These saccular contour defects also demonstrated apparent loss of the internal elastic lamina and apparent medial thinning (Fig. 3). These observations, which simulated microaneurysm formation, were a consequence of sectioning through the bases of perforating arteries. Localized loss of the IEL, apparently resulting from tissue tearing during processing and sectioning, was noticed either at the basilar terminus or adjacent to the basilar terminus in some sections (Fig. 4). Apart from these artifacts mentioned above, the IEL and media were intact and continuous along the distal basilar artery/P1 segments in all subjects. There were no bulge-like, local dilations to suggest microaneurysms or nascent aneurysm formation in any subject.

Discussion

Hemodynamically induced, intracranial aneurysms have been previously reported in rats, mice, and primates through carotid artery ligation [1–4]. Recently, Gao et al. [5] reported that, after either uni- or bilateral carotid artery ligation, microaneurysms were present at basilar terminus in all subjects at 12 weeks. More recently, that same group demonstrated same aneurysmal changes at the basilar terminus in all subjects as early as 5 days following carotid artery ligation [11, 12]. However, no in vivo imaging was provided in those studies and no gross imaging was discussed. In a previous study [6] by our own group, we prospectively performed histological evaluation of basilar tip up to 33 weeks following unilateral CCA ligation in rabbits. That previous study by our group did not utilize MICROFIL® but histologic findings were similar to what we report here.

The same MICROFIL® casting technique used in the current study has been confirmed to be an excellent technique to show the anatomy of the Circle of Willis and its branches in mice as compared to traditional microdissection [8]. Using the same technique along with MicroCT and mapping of histology, we successfully confirmed the microaneurysm formation (less than 50 μm) at the ACA in mice (unpublished data).

In the current study, we used the MICROFIL® technique matched with standard histological evaluation to explore the development of microaneurysm formation in the rabbit basilar terminus following RCCA ligation. We found no evidence of aneurysm formation in any subject. The correlation between MICROFIL®-opacified gross histology with consecutive histologic sections offers compelling evidence that the origins of perforating arteries may simulate microaneurysm formation in this model. Further, even minimal damage to tissue during processing may further simulate microaneurysm formation. While there remains no doubt that profound hemodynamic alterations result from carotid ligation, as evidenced by marked enlargement of the PComm ipsilateral to the ligated artery in our series, such hemodynamic alteration does not, in rabbits, lead to microaneurysm formation. These results indicate not only that unilateral carotid ligation in the rabbit should not be used to study intracranial aneurysm formation, but also that future studies of hemodynamically induced

microaneurysms, irrespective of species, should include MICROFIL® or and MicroCT studies.

There are several limitations in the current study. Only unilateral CCA ligation was performed and did not confirm whether there is aneurysm formation after bilateral CCA ligation. Second, we did not monitor the hemodynamic changes before and after unilateral RCCA ligation, since our study focused on the morphological change of basilar terminus wall. Finally, our conjecture regarding the role of tissue damage as a simulator of microaneurysm cannot be proved unequivocally.

Conclusions

Unilateral RCCA ligation does not induce microaneurysm formation at the basilar terminus in rabbits in our experience. Prominent perforating arteries as well as tissue injury from the processing may simulate “aneurysms” histologically.

Acknowledgments

This study was supported by a research grant from the National Institutes of Health (NIH NS42646).

References

1. Hashimoto N, Handa H, Nagata I, Hazama F. Experimentally induced cerebral aneurysms in rats: part V. Relation of hemo-dynamics in the Circle of Willis to formation of aneurysms. Surg Neurol. 1980; 13:41–45. [PubMed: 7361257]
2. Nagata I, Handa H, Hashimoto N, Hazama F. Experimentally induced cerebral aneurysms in rats: part VI. Hypertension. Surg Neurol. 1980; 14:477–479. [PubMed: 6111849]
3. Hashimoto NKC, Kikuchi H, Kojima M, Kang Y, Hazama F. Experimental induction of cerebral aneurysms in monkeys. J Neurosurg. 1987; 67:903–905. [PubMed: 3681429]
4. Morimoto M, Miyamoto S, Mizoguchi A, Kume N, Kita T, Hashimoto N. Mouse model of cerebral aneurysm. Experimental induction by renal hypertension and local hemodynamic changes. Stroke. 2002; 33:1911–1915. [PubMed: 12105374]
5. Gao L, Hoi Y, Swartz DD, Kolega J, Siddiqui A, Meng H. Nascent aneurysm formation at the basilar terminus induced by hemodynamics. Stroke. 2008; 39:2085–2090. [PubMed: 18451348]
6. Dai D, Ding YH, Kadirvel R, Lewis DA, Kallmes DF. Experience with microaneurysm formation at the basilar terminus in the rabbit elastase aneurysm model. AJNR Am J Neuroradiol. 2009; 31:300–303. [PubMed: 19797794]
7. Dai D, Kallmes DF. Aneurysmal changes at the basilar terminus in the rabbit elastase aneurysm model: reply. AJNR Am J Neuroradiol. 2010; 31:E37.
8. Abruzzo T, Tumialan L, Chaalala C, Kim S, Guldberg RE, Lin A, Leach J, et al. Microscopic computed tomography imaging of the cerebral circulation in mice: feasibility and pitfalls. Synapse. 2008; 62:557–565. [PubMed: 18509853]
9. Altes TA, Cloft HJ, Short JG, DeGast A, Do HM, Helm GA, et al. 1999 ARRS Executive Council Award. Creation of saccular aneurysms in the rabbit: a model suitable for testing endovascular devices. American Roentgen Ray Society. AJR Am J Roentgenol. 2000; 174:349–354. [PubMed: 10658703]
10. Ding YH, Danielson MA, Kadirvel R, Dai D, Lewis DA, Cloft HJ, et al. Modified technique to create morphologically reproducible elastase-induced aneurysms in rabbits. Neuroradiology. 2006; 48:528–532. [PubMed: 16708202]
11. Metaxa E, Tremmel M, Natarajan SK, Xiang J, Paluch RA, Mandelbaum M, et al. Characterization of critical hemodynamics contributing to aneurysmal remodeling at the basilar terminus in a rabbit model. Stroke. 2010; 41:1774–1782. [PubMed: 20595660]

12. Tremmel MXJ, Hoi Y, Kolega J, Siddiqui AH, Mocco J, Meng H. Mapping vascular response to in vivo hemodynamics: application to increased flow at the basilar terminus. Biomech Model Mechanobiol. 2010; 9:421–434. [PubMed: 20054605]

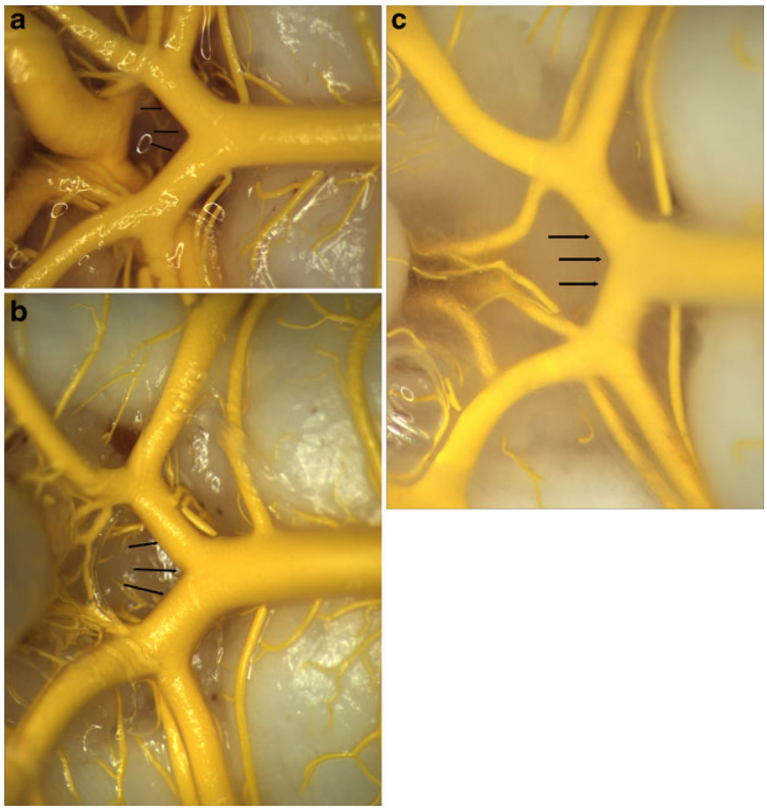

Fig. 1.

Gross photo of MICROFIL®-filled basilar arteries and its branches. **a** and **b** Harvested at 0 day (**a**) and 16 weeks (**b**) after right common carotid ligation; **c** is from the control group. **a**–**c** All show the local arterial wall at the basilar terminus (*arrow*) appear to be smooth and even, without evidence of local dilation or bulge formation

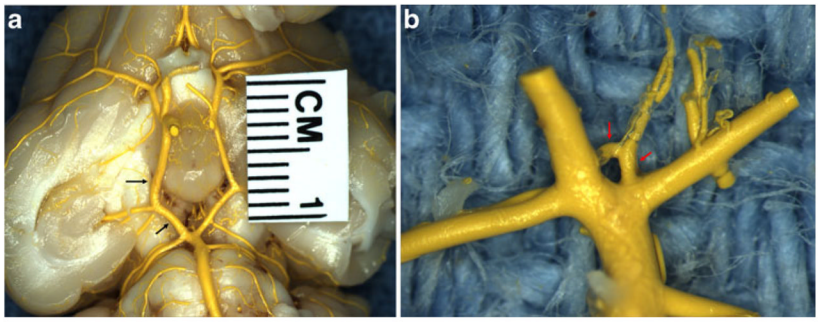

Fig. 2.

Gross photo of MICROFIL®-filled cerebral arteries harvested at 3 weeks after right common carotid ligation. **a** Shows the entire Circle of Willis. Note asymmetric enlargement of the right posterior communicating artery (*arrow*). **b** The high magnification of basilar terminus and its branches, showing prominent perforating arteries at the basilar terminus area (*arrow*)

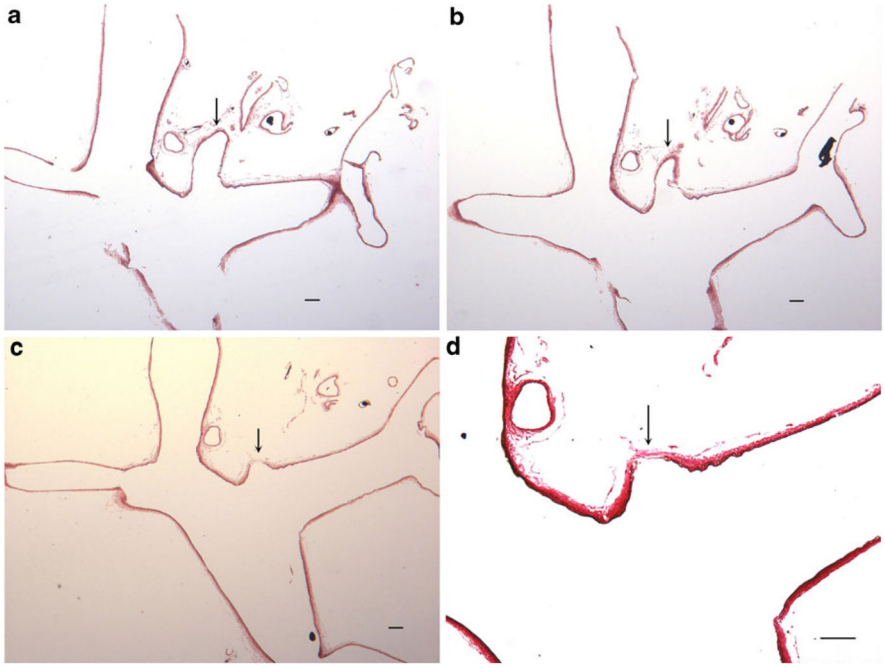

Fig. 3.

Serial histological sections of basilar terminus and one of its branches from the subject in Fig. 1. **a**, **b** Serial sections showing the branch at the BT (*arrow*) (hematoxylin and eosin (H&E), original magnification ×40). **c**, **d** Serial section of **a** and **b**, showing the base of a branch at the BT, demonstrating apparent internal elastic lamella loss and media thinning at the base of a perforating branch, which mimics the morphological appearance of an aneurysm (*arrows* in **c** and **d**) (**c**, H&E, original magnification ×40; **d**, high magnification of **c**, Verhoeff Van Gieson, original magnification ×100). *Bar*=100 μm

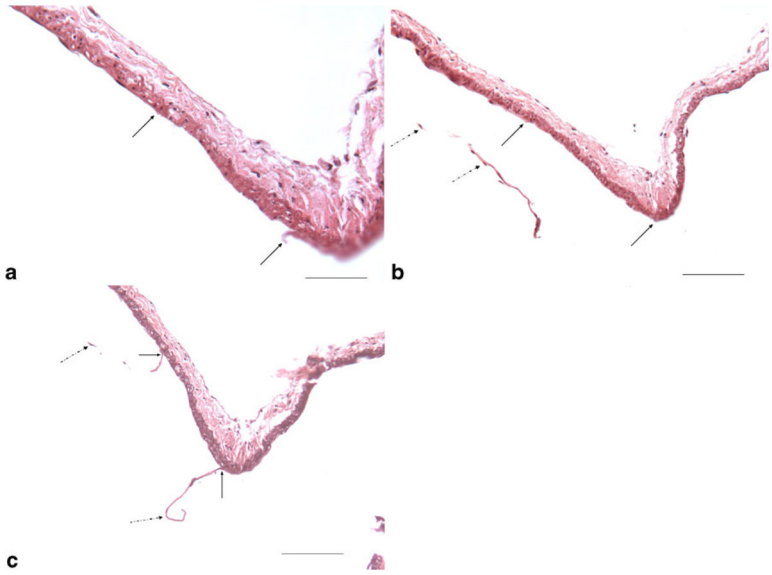

Fig. 4.

Serial sections from one 16-week subject illustrate artifact damage to the internal elastic lamella and endothelial cells (EC) during processing. **a** Showing local, sharp IEL and EC loss from processing (between two *arrows*) (H&E, original magnification ×400, *bar*=50 μm); **b**, **c** adjacent serial sections from the same subject as (**a**), showing the local IEL and EC loss (between two *black arrows*) at the same location in (**a**), as well the torn IEL and EC (*dashed black arrows*) (H&E, original magnification ×200, *bar*=100 μm)